HHS Public Access

Author manuscript

J Endocrinol. Author manuscript; available in PMC 2022 September 20.

Published in final edited form as:

J Endocrinol. ; 251(2): 125–135. doi:10.1530/JOE-20-0612.

Loss of ARC Worsens High Fat Diet-Induced Hyperglycemia in Mice

Andrew T. Templin[1], **Christine Schmidt**[1], **Meghan F. Hogan**[1], **Nathalie Esser**[1], **Richard N. Kitsis**[2], **Rebecca L. Hull**[1], **Sakeneh Zraika**[1], **Steven E. Kahn**[1]

[1]Department of Medicine, Division of Metabolism, Endocrinology and Nutrition, Veteran Affairs Puget Sound Health Care System and University of Washington, Seattle, WA, USA

[2]Departments of Medicine and Cell Biology and Wilf Family Cardiovascular Research Institute, Albert Einstein College of Medicine, Bronx, NY, USA

Abstract

Apoptosis repressor with caspase recruitment domain (ARC) is an endogenous inhibitor of cell death signaling that is expressed in insulin-producing β cells. ARC has been shown to reduce β-cell death in response to diabetogenic stimuli *in vitro*, but its role in maintaining glucose homeostasis *in vivo* has not been fully established. Here we examined whether loss of ARC in FVB background mice exacerbates high fat diet (HFD)-induced hyperglycemia *in vivo* over 24 weeks. Prior to commencing 24-week HFD, $ARC^{-/-}$ mice had lower body weight than wild type (WT) mice. This body weight difference was maintained until the end of the study and was associated with decreased epididymal and inguinal adipose tissue mass in $ARC^{-/-}$ mice. Non-fasting plasma glucose was not different between $ARC^{-/-}$ and WT mice prior to HFD feeding, and $ARC^{-/-}$ mice displayed a greater increase in plasma glucose over the first 4 weeks of HFD. Plasma glucose remained elevated in $ARC^{-/-}$ mice after 16 weeks of HFD feeding, at which time it had returned to baseline in WT mice. Following 24 weeks of HFD, non-fasting plasma glucose in $ARC^{-/-}$ mice returned to baseline and was not different from WT mice. At this final time point, no differences were observed between genotypes in plasma glucose or insulin under fasted conditions or following IV glucose administration. However, HFD-fed $ARC^{-/-}$ mice exhibited significantly decreased β-cell area compared to WT mice. Thus, ARC deficiency delays, but does not prevent, metabolic adaptation to HFD feeding in mice, worsening transient HFD-induced hyperglycemia.

Keywords

ARC; diabetes; islet; β cell; cell death

Corresponding Author: Steven E. Kahn, VA Puget Sound Health Care System (151), 1660 S. Columbian Way, Seattle, WA 98108, Telephone: 206-277-5515, Fax: 206-764-2164, skahn@uw.edu.

AUTHOR CONTRIBUTION STATEMENT: A.T.T. participated in study design, performed research, analyzed and interpreted data, and wrote the manuscript. C.W.S., M.F.H. and N.E. participated in study design, performed research, analyzed and interpreted data, and revised/approved the manuscript. R.N.K., R.L.H., S.Z. and S.E.K. participated in study design, analyzed and interpreted data, and revised/approved the manuscript. A.T.T. and S.E.K. are responsible for the integrity of the work as a whole.

DECLARATION OF INTEREST: The authors declare that there is no conflict of interest that could be perceived as prejudicing the impartiality of the research reported.

INTRODUCTION

Apoptosis repressor with caspase recruitment domain (ARC), the protein product of the nucleolar protein 3 (*Nol3*) gene, is an endogenous, multifunctional inhibitor of cell death (Koseki et al., 1998; Nam et al., 2004; Davis et al., 2013; Jang et al., 2015). ARC's N-terminal caspase recruitment domain (CARD) has been shown to interact with and inhibit numerous effectors of cell death (Davis et al., 2013; Geertman et al., 1996; Jang et al., 2015; Koseki et al., 1998). Originally, ARC was shown to interact with caspase 2 and 8 and to prevent cardiac and skeletal muscle cell death (Jo et al., 2004; Koseki et al., 1998). Subsequent work demonstrated ARC inhibits other effectors of cell death including Bax, Bad and p53, and that inhibition of these molecules was similarly mediated through interactions with ARC's CARD (Davis et al., 2013; Gustafsson et al., 2004; Li et al., 2008). Moreover, ARC has been shown to diminish TNFα-induced regulated necrosis, further illustrating its multifunctional role in mitigating cell death (Kung et al., 2014). ARC has also been identified in insulin-producing islet β cells (McKimpson et al., 2013). Given its presence in β cells, which produce insulin to regulate glucose utilization, and in skeletal muscle, a primary tissue for peripheral glucose uptake and disposal, ARC is well-placed to influence whole-body glucose homeostasis.

In vitro studies have demonstrated that ARC reduces β-cell death in response to palmitate and chemically-induced endoplasmic reticulum (ER) stress (McKimpson et al., 2013) as well as to endogenous islet amyloid formation (Templin et al., 2017), these being β-cell stressors associated with the pathogenesis of type 2 diabetes (T2D) (Back and Kaufman, 2012; Hull et al., 2004; Jurgens et al., 2011; Özcan et al., 2004). Despite its potential to prevent β-cell loss, few studies have examined ARC's role in maintaining whole-body glucose homeostasis *in vivo*. McKimpson and colleagues showed that genetic ARC deficiency did not alter islet morphology or impair glucose homeostasis *in vivo* in C57BL/6 mice fed a normal chow diet (NCD) (McKimpson et al., 2017). However, loss of ARC in leptin deficient (*ob/ob*) mice that are hyperphagic, obese, insulin resistant and hyperglycemic was found to increase β-cell death, impair glucose-stimulated insulin secretion and exacerbate hyperglycemia (McKimpson et al., 2017). These findings were the first to show that ARC is required for β-cell survival and sufficient insulin secretion *in vivo* in response to a genetic model of diabetogenic stress.

The role of ARC in β-cell adaptation to high fat diet (HFD) feeding, a physiologically relevant metabolic stress, remains unknown. HFD feeding is a metabolic challenge that leads to weight gain, insulin resistance and subsequent β-cell compensation to increase insulin secretion and maintain glucose homeostasis (Gupta et al., 2017; Mosser et al., 2015; Paschen et al., 2019). This challenge is commonly used to test β-cell functional capacity and glucose homeostasis when examining metabolic phenotypes in knockout mouse models (Surwit et al., 1988; Ikemoto et al., 1996; Asghar et al., 2006; Heydemann, 2016; Hull et al., 2017). We hypothesized that loss of ARC would diminish β-cell compensation in response to HFD feeding, leading to impaired insulin secretion and worsened hyperglycemia in ARC deficient mice. To address this hypothesis, we examined glycemic status, β-cell function and β-cell area in mice with or without whole-body genetic loss of ARC that were fed a NCD or a HFD for 24 weeks.

MATERIALS AND METHODS

Animals

Heterozygous ARC$^{+/-}$ mice on an FVB background were obtained from Richard N. Kitsis (Albert Einstein College of Medicine, Bronx, NY) and maintained as ARC$^{+/+}$ (WT) and ARC$^{-/-}$ breeding lines for this study. All mice used in this study were less than 5 generations post-divergence from ARC$^{+/-}$ mice. Mice were housed and bred in a specific-pathogen-free vivarium at VA Puget Sound Health Care System (VAPSHCS) with *ad libitum* access to food and water. Male mice of the indicated ages were studied. All procedures were approved by the VAPSHCS Institutional Animal Care and Use Committee.

Genotyping

Polymerase chain reaction (PCR) of tail DNA using specific primers was used to determine the presence of *Nol3* WT and mutant alleles. Amplification of these alleles was performed using the following primers to generate 400 bp WT products and 600 bp mutant products: forward, 5'-TTCCTACGGTTTGGTACAGGCA-3'; reverse, 5'-TGGTACACCAAGCCGAGTGATT-3'; mutant, 5'-CCTGCCAGAGCTTGACCCCA −3'.

Islet isolation and quantitative real-time reverse transcription PCR (qRT-PCR)

Islets from 8–12 week old WT and ARC$^{-/-}$ mice were isolated by collagenase P digestion, then recovered overnight in RPMI 1640 medium containing 10% fetal bovine serum, 1 mM sodium pyruvate, 100 units/ml penicillin, 100 μg/ml streptomycin and 11.1 mM glucose. The following day, islets from each genotype were lysed and total RNA was recovered using the High Pure RNA Isolation Kit (Roche, Basel, Switzerland). RNA was then reverse transcribed and subjected to qRT-PCR. Loss of *Nol3* mRNA in ARC$^{-/-}$ islets was confirmed using Taqman probes (ThermoFisher Scientific, Waltham, MA) to quantify expression of *Nol3* mRNA (Mm07299538_g1) and 18S rRNA (HS99999901_s1), with data normalized to 18S rRNA levels and expressed as fold relative to WT mice. All qRT-PCR data points represent means of triplicate determinations.

In vivo studies

NCD fed mice consumed food containing 21% kcal from fat (LabDiet, PicoLab 5058, St. Louis, MO) from weaning until analysis at 16- or 35-weeks-of-age. HFD fed mice consumed food containing 60% kcal from fat (Research Diets, #D12492N, New Brunswick, NJ) for 24 weeks, starting at 10–12 weeks of age and ending at 34–36 weeks of age.

Tissue collection, histology and quantitative microscopy

Mice were euthanized and pancreas, liver, epididymal adipose, inguinal adipose, brown adipose, gastrocnemius muscle and vastus medialis muscle tissue were excised, and mass was recorded. After excision, pancreases were fixed in 4% (wt/vol) phosphate-buffered paraformaldehyde, processed and embedded in paraffin. To visualize β cells, 4 μm pancreas sections were cut and stained with mouse monoclonal anti-insulin antibody (I-2018, 1:2000, Sigma-Aldrich, St. Louis, MO) followed by goat anti-mouse Alexa Fluor 488 (#A-11001, Life Technologies, Carlsbad, CA, 1:200). To visualize α cells, sections were incubated

with rabbit monoclonal anti-glucagon antibody (#Ab92517, Abcam, Cambridge, UK; 1:100) followed by goat anti-rabbit Alexa Fluor 546 (#A-11010, Life Technologies, Carlsbad, CA, 1:200). Sections were mounted with polyvinyl alcohol containing Hoechst 33258 to visualize nuclei. Islet area, β-cell area and α-cell area were imaged with a fully automated NiE microscope (Nikon, Tokyo, Japan) equipped with NIS Elements High Content software and automated JOBS-based acquisition and analysis algorithms (NIS Elements, Nikon, Tokyo, Japan). Islet images were captured at 20X magnification, then insulin and glucagon-positive area was quantified using automated analysis software (NIS Elements, Nikon). Binary layers for insulin and glucagon were used in post-processing steps to calculate total islet area, then insulin-positive and glucagon-positive areas were calculated on a per islet basis. All islets visible on each section were quantified, with an average of 34 ± 2 islets analyzed per replicate per condition. Ki67 and cleaved caspase 3 staining and analysis was performed by automated immunohistochemistry through the University of Washington Diabetes Research Center's Cellular and Molecular Imaging Core using antibodies specific to Ki67 (clone D3B5, Cell Signaling, #12202), and cleaved caspase 3 (clone D3E9, Cell Signaling, #9579). Antibody complexes were visualized using DAB (3,3'-diaminobenzidine) and slides were counterstained with hematoxylin. Slides were scanned with a 20X objective using NanoZoomer Digital Pathology System (Hamamatsu City, Japan) and digital images were imported into Visiopharm software (Hoersholm, Denmark) for analysis. The Visiopharm software was trained to label positive staining for Ki67, cleaved caspase 3 and background counterstain (hematoxylin) using a project specific configuration. Observers were blinded to genotype of the pancreas section for all quantitative microscopy.

Intravenous glucose tolerance tests

Mice were fasted for 16 hours, then anesthetized with intraperitoneal sodium pentobarbital for the duration of the procedure. Under anesthesia, a catheter was placed in the carotid artery and glucose was administered at a dose of 1 g/kg body weight, after which the catheter was flushed with heparinized saline. Blood was sampled 5 minutes before (fasting sample) and 2, 5, 10, 20, 30 and 45 minutes after glucose administration for measurement of plasma glucose and insulin. Following the 10, 20 and 30 minute blood draws, red blood cells were resuspended in heparinized saline and reinfused via carotid artery to prevent hypovolemic/anemic shock. First- and second-phase insulin secretion were calculated as the ratio of incremental area under the curve (iAUC) for insulin over iAUC glucose for 0–5 minutes and for 5–45 minutes, respectively.

Insulin tolerance tests

Mice were fasted for 4 hours and a baseline blood sample was taken via tail vein. Insulin was injected intraperitoneally at a dose of 1 U/kg body weight, and plasma glucose was measured at 0, 15, 30 and 60 minutes after insulin administration using a handheld glucometer (Accu-Chek, Roche, Basel, Switzerland) on blood samples obtained via tail tip.

Glucose and insulin assays

Plasma was separated from blood by centrifugation and stored at -30^0C for subsequent analysis. Plasma glucose concentrations were determined using a plate based colorimetric

assay utilizing the glucose oxidase method, and plasma insulin concentrations were determined using an ultrasensitive mouse insulin ELISA assay (#80-INSMSU-E10, ALPCO, Salem, NH, USA). Each measure represents the mean of triplicate determinations.

Statistical analyses

Normality of data distribution in each data set was tested using the D'Agostino-Pearson normality test. Normally distributed data were analyzed using two-tailed Student's t-tests, while non-normally distributed data were analyzed using Mann-Whitney U tests. Longitudinal data were analyzed using repeated measures two-way analysis of variance (ANOVA), with significant results followed by Fisher's Least Significant Difference (LSD) post-hoc analysis of specific time points. No outliers were excluded from the data sets presented. Statistical analyses were conducted with GraphPad Prism 8 software (GraphPad, San Diego, CA). Data are presented as mean ± standard error, with a value of $p<0.05$ considered significant.

RESULTS

ARC$^{-/-}$ mice fed NCD do not display alterations in islet, β-cell, or α-cell area at 16 or 35 weeks of age

We first examined WT and ARC$^{-/-}$ mice fed NCD. At 16 weeks of age, we observed significantly reduced body weight in ARC$^{-/-}$ mice (Fig. 1A), but no difference in average islet area (Fig. 1B), β-cell area (Fig. 1C) or α-cell area (Fig. 1D) were found between WT and ARC$^{-/-}$ mice. At 35 weeks of age, we found a trend towards reduced body weight in ARC$^{-/-}$ mice (Fig. 2A, $p=0.09$), and again observed no difference in average islet area (Fig. 2B), β-cell area (Fig. 2C) or α-cell area (Fig. 2D) between genotypes. However, WT mice displayed a significant increase in islet size from 16 to 35 weeks (from 14259 ± 1786 μm^2 to 25328 ± 3547 μm^2, $p=0.04$), whereas islet size in ARC$^{-/-}$ did not differ over this period (13626 ± 1137 μm^2 vs. 18304 ± 2842 μm^2, $p=0.22$). Loss of ARC mRNA expression (*Nol3*) was confirmed in ARC$^{-/-}$ isolated islets (Fig. 1E). Representative images of islets from 16 (Fig. 1F) and 35 (Fig. 2E) week old WT and ARC$^{-/-}$ mice are displayed.

ARC$^{-/-}$ mice fed NCD display normal glucose homeostasis and insulin secretion at 35 weeks of age

35-week old ARC$^{-/-}$ mice exhibited no difference in fasting plasma glucose (Fig. 3A) or fasting plasma insulin (Fig. 3B) compared to WT mice. Following intravenous glucose administration, neither plasma glucose (Fig. 3C) nor insulin (Fig. 3D) differed in ARC$^{-/-}$ compared to WT mice. First-phase and second-phase insulin secretion were not different between 35-week-old WT and ARC$^{-/-}$ mice, as measured by incremental area under the curve (iAUC) of insulin/iAUC glucose from 0 to 5 (Fig. 3E) or 5 to 45 (Fig. 3F) minutes, respectively.

ARC$^{-/-}$ mice exhibit worsened HFD-induced hyperglycemia

We next began a 24-week high fat diet (HFD) feeding study of WT and ARC$^{-/-}$ mice ending at 35 weeks of age. When analyzed over the full 24-week HFD feeding period, ARC$^{-/-}$ mice exhibited higher plasma glucose levels compared to WT mice (Fig. 4A, $p<0.05$).

Non-fasting plasma glucose was not different between groups prior to HFD (Fig. 4A). From baseline, ARC$^{-/-}$ mice displayed a greater increase in plasma glucose after 4 weeks of HFD feeding compared to WT mice (55.8 ± 20.5 mg/dl vs. 2.2 ± 9.4 mg/dl, p=0.03, Fig. 4B). Plasma glucose rose to equivalent absolute levels in ARC$^{-/-}$ and WT mice after 8 weeks of HFD feeding. After 16 weeks of HFD, ARC$^{-/-}$ mice displayed significantly higher absolute plasma glucose (244.0 ± 8.5 mg/dl vs. 178.0 ± 6.4 mg/dl, p<0.001, Fig. 4A) and change in plasma glucose (62.62 ± 13.99 mg/dl vs. −22.60 ± 8.04 mg/dl, p<0.001, Fig. 4B) compared to WT mice. After 24 weeks of HFD, the observed difference in plasma glucose was no longer present (Fig. 4A, B), although ARC$^{-/-}$ mice exhibited a trend for increased change in plasma glucose at this time (18.0 ± 12.9 vs. −8.4 ± 6.1 mg/dl, p=0.08, Fig. 4B).

ARC$^{-/-}$ mice display reduced body weight but equivalent weight gain in response to HFD

At 10–12 weeks of age before HFD feeding began, ARC$^{-/-}$ mice had lower body weight than WT mice (26.2 ± 0.6 g vs. 30.6 ± 0.8 g, p<0.001, Fig. 4C), and this difference in body weight remained until the end of the 24-week HFD study (40.9 ± 1.7 g vs. 46.8 ± 1.6 g, p=0.02, Fig. 4C). However, the degree of body weight gain due to HFD was not different between WT and ARC$^{-/-}$ mice (Fig. 4D). Vastus medialis muscle, epididymal adipose and inguinal adipose tissue mass were decreased in ARC$^{-/-}$ compared to WT mice (Figs. 4E, F), but no differences in pancreas, liver, gastrocnemius muscle or brown adipose tissue mass were observed between genotypes (Figs. 4E, F).

ARC$^{-/-}$ mice fed HFD display reduced β-cell area but no differences in α-cell area, islet area, proliferation or apoptosis compared to WT mice after 24 weeks of HFD

Following 24 weeks of HFD feeding, ARC$^{-/-}$ mice had decreased β-cell area compared to WT mice (72.69 ± 1.83% vs. 77.32 ± 1.27% insulin/islet area, p=0.04, Fig. 5A). No difference in α-cell area existed at this timepoint (3.33 ± 0.73% vs. 2.94 ± 0.44% glucagon/islet area, p=0.64, Fig. 5B,), but a trend towards reduced islet area was observed in ARC$^{-/-}$ mice (28111.5 ± 4355.33 μm^2 vs. 39292.7 ± 4021.7 μm^2, p=0.07, Fig. 5C). Ki67 expression tended to be increased in ARC$^{-/-}$ pancreas sections (p=0.06, Fig. 5D), while cleaved caspase 3 expression was unaltered (p=0.27, Fig. 5E) following HFD feeding.

ARC$^{-/-}$ mice display unaltered glucose homeostasis, insulin secretion and insulin sensitivity after 24 weeks of HFD

At the end of the HFD feeding period, ARC$^{-/-}$ mice exhibited no difference in fasting plasma glucose (Fig. 6A, 127.5 ± 12.0 mg/dl vs. 117.3 ± 6.9 mg/dl, p=0.49) or fasting plasma insulin (Fig. 6B, 181.48 ± 33.65 pM vs. 221.57 ± 63.39 pM, p=0.57) compared to WT mice. Upon challenge with intravenous glucose, neither plasma glucose (Fig. 6C) nor insulin (Fig. 6D) differed in ARC$^{-/-}$ compared to WT mice. The incremental area under the curve (iAUC) of insulin/iAUC glucose was not significantly different from 0 to 5 minutes (Fig. 6E, 2.90 ± 0.35 vs. 4.13 ± 0.86, p=0.19) or 5 to 45 minutes (Fig. 6F, 1.96 ± 0.40 vs. 2.76 ± 0.80, p=0.37). Furthermore, no difference in insulin sensitivity was observed between WT and ARC$^{-/-}$ mice after the HFD feeding period as measured by intraperitoneal insulin tolerance test (Figs. 6G, H).

DISCUSSION

ARC plays an important role in regulating cell death signaling (Koseki et al., 1998; Neuss et al., 2001) in multiple cell types, including insulin-producing islet β cells (McKimpson et al., 2017, 2013; Templin et al., 2017). Given that β-cell loss can contribute to the development of insulin secretory dysfunction and hyperglycemia (Butler et al., 2003; Rahier et al., 2008), ARC has attracted attention as a molecule that could be targeted to maintain β-cell survival and function to prevent diabetes. In this study we used a mouse model of whole-body genetic ARC deficiency ($ARC^{-/-}$) to examine, for the first time, whether loss of ARC impairs metabolic adaptation to the physiologically relevant stress of HFD feeding and, if so, whether β-cell loss and insulin secretory dysfunction contribute to this phenotype.

We found that $ARC^{-/-}$ mice on a FVB background fed a NCD displayed reduced body weight, but unaltered β-cell area and glucose homeostasis compared to their WT counterparts. In contrast, $ARC^{-/-}$ mice challenged with HFD for 24-weeks exhibited accelerated and prolonged hyperglycemia along with lower body weight throughout this interval. By the end of the HFD feeding period, however, hyperglycemia had resolved in $ARC^{-/-}$ mice. Thus, our data indicate that ARC deficiency delays, but does not prevent, metabolic adaptation to HFD feeding in mice, worsening transient HFD-induced hyperglycemia.

While this study is the first to examine how loss of ARC impacts metabolic adaptation to HFD feeding, McKimpson and colleagues (McKimpson et al., 2017) previously challenged $ARC^{-/-}$ mice using the *ob/ob* model of leptin deficiency, marked obesity, insulin resistance and hyperglycemia. In both our study and theirs, unchallenged $ARC^{-/-}$ mice were found to exhibit normal glucose metabolism and islet morphology. However, when *ob/ob* and $ARC^{-/-}$ mice were crossed, the resulting mice (*ob/ob*;$ARC^{-/-}$) demonstrated significantly increased non-fasting glucose, reduced β-cell area, glucose intolerance, impaired glucose-stimulated insulin secretion (GSIS) and reduced insulin sensitivity compared to *ob/ob* mice alone (McKimpson et al., 2017). In contrast to this earlier study, when we challenged $ARC^{-/-}$ mice with the milder and more physiologically relevant metabolic stress of HFD feeding, we observed a less severe metabolic phenotype. Similar to *ob/ob*;$ARC^{-/-}$ mice, our $ARC^{-/-}$ mice exhibited significantly increased non-fasting glucose and reduced terminal β-cell area compared to their WT counterparts. However, HFD-induced hyperglycemia resolved in both WT and $ARC^{-/-}$ mice by the end of the 24-week HFD feeding period, and at this time $ARC^{-/-}$ mice exhibited unaltered glucose tolerance, GSIS and insulin sensitivity. Thus, the differing metabolic challenges applied to $ARC^{-/-}$ mice in these studies likely resulted in different phenotypic outcomes, with $ARC^{-/-}$ mice exhibiting a delayed but intact ability to adapt metabolically to HFD feeding. Together, these studies indicate that ARC deficiency alone does not cause β-cell loss or hyperglycemia *in vivo*, but loss of ARC exacerbates hyperglycemia in response to metabolic challenges such as HFD feeding and genetically-induced obesity and insulin resistance.

We found that $ARC^{-/-}$ mice exhibited significantly reduced body weight compared to WT mice both at baseline and over 24 weeks of HFD feeding. We also observed that β-cell area was reduced in $ARC^{-/-}$ mice at the end of HFD feeding, a time when plasma glucose,

glucose tolerance and GSIS did not differ from WT mice. Additionally, our data show that cleaved caspase 3, a marker of apoptosis, was not increased in $ARC^{-/-}$ pancreases at this time point, while Ki67, a marker of proliferation, tended to be increased. Thus, we do not believe the reduced β-cell area observed in $ARC^{-/-}$ mice in our study is pathological, but rather the result of lower body weight and reduced β-cell secretory demand elicited from HFD feeding.

The body weight phenotype we identified in $ARC^{-/-}$ mice in this study was not observed in McKimpson et al.'s study of $ARC^{-/-}$ mice (McKimpson et al., 2017). This difference between studies could have arisen due to the different genetic backgrounds used in these studies, with the present study examining mice on an FVB background and the previous work using mice on a C57Bl/6 (B6) background. While B6 mice are prone to obesity, insulin resistance and glucose intolerance, FVB mice (also known as 129) are relatively resistant to these phenotypes (Almind and Kahn, 2004; Champy et al., 2008; Tschöp et al., 2011). This resistance to obesity in FVB compared to B6 mice is related to higher metabolic rate, while caloric intake on a HFD is similar between backgrounds (Almind and Kahn, 2004). Therefore, it is possible that effects of ARC deficiency on metabolic rate or energy expenditure were more pronounced in our study using FVB mice, and that these effects underly the body weight phenotype we observed. Although we did not collect food intake data in this study, McKimpson et al. previously found that food intake was increased by ~30% in $ARC^{-/-}$ mice compared to mice with intact ARC expression on an *ob/ob* background (McKimpson et al., 2017), suggesting reduced food intake is not likely to explain the lower body weight observed in $ARC^{-/-}$ mice in our study.

Several different HFD experimental designs have been used to induce metabolic dysfunction in mice, with these designs eliciting varying degrees of insulin resistance, hyperglycemia and insufficient insulin secretion (Mosser et al., 2015; Winzell and Ahrén, 2004). Over a period of months, metabolic adaptation to the diet takes place so that hyperglycemia generally resolves (Mosser et al., 2015; Winzell and Ahrén, 2004). This adaptation includes expansion of β-cell mass and function to increase insulin secretion and restore plasma glucose levels to normal (Ahrén et al., 2010; Gupta et al., 2017). We observed that HFD-induced hyperglycemia was accelerated and prolonged in $ARC^{-/-}$ mice, and that resolution of this hyperglycemia occurred after 24 weeks of HFD feeding vs. after 16 weeks in WT mice. $ARC^{-/-}$ mice also displayed decreased β-cell area after 24 weeks of HFD compared to WT mice. Although we did not measure plasma insulin after 16 weeks of HFD, it appears plausible that loss of ARC in the β-cell impaired expansion of β-cell mass and function in response to HFD and contributed to the worsened hyperglycemia observed in $ARC^{-/-}$ mice at this time point. However, at completion of HFD feeding $ARC^{-/-}$ mice exhibited unaltered GSIS, and when compared to NCD fed mice of the same age, HFD increased maximal intravenous GSIS by 39% in WT mice versus 35% in $ARC^{-/-}$ mice. Given the similar stimulation of insulin responses by HFD between genotypes, our data do not suggest failed β-cell compensation in $ARC^{-/-}$ mice at the end of the study.

One link between ARC's mechanism of action and β-cell adaptation to HFD is found in endoplasmic reticulum (ER) homeostasis. As demand for β-cell insulin production increases, cells undergo an adaptive response to facilitate increased insulin biosynthesis

in part by expanding ER size (Marchetti et al., 2007), and this process has been shown to occur in association with obesity and β-cell compensation (Omikorede et al., 2013). When this adaptive response is inadequate to meet insulin demand, ER stress signaling initiates cell death pathways, and ARC is involved in this process (McKimpson et al., 2017, 2013). Previous *in vitro* studies showed that ARC overexpression reduces β-cell death and ARC knockdown increases β-cell death in response to thapsigargin-induced ER stress (McKimpson et al., 2013). Although we have not assessed ER stress in ARC$^{-/-}$ islets in the present study, we believe ARC's role in maintaining β-cell ER homeostasis could have contributed to the transient worsening of HFD-induced hyperglycemia observed in ARC$^{-/-}$ mice.

Given our use of whole-body ARC$^{-/-}$ mice, it is difficult to ascribe the phenotype we observed to loss of ARC in any specific tissue. Generation and study of β-cell specific ARC knockout mice would aid in defining ARC's role in β-cell homeostasis in the future. As for the present study, we acknowledge that loss of ARC in tissues other than the β cell may have contributed to the reduced body weight and exacerbated HFD-induced hyperglycemia we observed in ARC$^{-/-}$ mice. Primary among these tissues are insulin sensitive peripheral tissues involved in glucose homeostasis and disposal such as liver, skeletal muscle and adipose tissue in which ARC is expressed (Koseki et al., 1998; Charron et al., 1989; De et al., 1988; An et al., 2013; Rosell et al., 2014). After 24 weeks of HFD feeding, ARC$^{-/-}$ mice exhibited decreased epididymal and inguinal adipose tissue mass, as well as reduced vastus medialis muscle mass. This reduction in mass may have been due to increased cell death in the absence of ARC, as has been reported in skeletal muscle (Davis et al., 2013; Koseki et al., 1998). One would hypothesize that decreased adipose tissue mass in ARC$^{-/-}$ mice would have resulted in improved insulin sensitivity and glucose tolerance, but we did not observe such improvements in this study. Although studies have shown that ARC is expressed in white and brown adipose tissue depots (Liu et al., 2015; Min et al., 2019; Rosell et al., 2014), relatively little is known about the role of ARC in adipose tissue. Thus, it is possible that loss of ARC in adipose tissue impacts glucose homeostasis. Additional studies utilizing models of tissue specific ARC deficiency are needed to understand ARC's role in regulating metabolism in insulin sensitive peripheral tissues.

In summary, we demonstrated that unchallenged whole-body ARC$^{-/-}$ mice on an FVB background exhibit reduced body weight, but no alterations in islet morphology, glucose tolerance or GSIS compared to WT mice *in vivo*. In contrast, when challenged with 24 weeks of HFD feeding, ARC$^{-/-}$ mice displayed decreased body weight, but exhibited accelerated and prolonged hyperglycemia compared to WT mice. By the end of the study, ARC$^{-/-}$ mice had undergone metabolic adaptation to HFD feeding similar to WT mice, with no alterations in plasma glucose or plasma insulin observed in either the fasted or glucose-stimulated state, but with decreased β-cell area. Our study shows that ARC promotes early metabolic adaptation to HFD feeding, and as such is a molecule that could be targeted to maintain glucose homeostasis in the setting of T2D.

ACKNOWLEDGEMENTS:

We thank R. N. Kitsis (Albert Einstein College of Medicine, Bronx, NY) for providing $ARC^{+/-}$ mice on an FVB background. We thank B. Barrow, B. Fountaine, D. Hackney and S. Mongovin (Seattle Institute for Biomedical and Clinical Research, Seattle, WA, USA), and B. Johnson and S. Lindhartsen (University of Washington Diabetes Research Center Cellular and Molecular Imaging Core) for excellent technical assistance provided during the performance of these studies. Some of the data from this study were presented in abstract form at the American Diabetes Association 80^{th} Scientific Sessions in 2020.

FUNDING: This work was supported by funding from the U.S. Department of Veterans Affairs (IK2 BX004659 to A.T.T., I01 BX004063 to R.L.H., I01 BX001060 to S.E.K.), National Institutes of Health (P30 DK017047 to the University of Washington Diabetes Research Center; F32 DK109584 to M.F.H.; R01 DK098506 to S.Z.), American Diabetes Association (Mentor-Based Fellowship to S.E.K.; Postdoctoral Fellowship 1-18-PDF-174 to M.F.H.), University of Washington (McAbee Fellowship to M.F.H. and N.E.), and French Society of Diabetes (to N.E.).

REFERENCES

Ahrén J, Ahrén B, Wierup N, 2010. Increased β-cell volume in mice fed a high-fat diet: A dynamic study over 12 months. Islets 2, 353–356. 10.4161/isl.2.6.13619 [PubMed: 21099337]

Almind K, Kahn CR, 2004. Genetic Determinants of Energy Expenditure and Insulin Resistance in Diet-Induced Obesity in Mice. Diabetes 53, 3274–3285. 10.2337/diabetes.53.12.3274 [PubMed: 15561960]

An J, Mehrhof F, Harms C, Lättig-Tünnemann G, Lee SLL, Endres M, Li M, Sellge G, Mandić AD, Trautwein C, et al. , 2013. ARC is a novel therapeutic approach against acetaminophen-induced hepatocellular necrosis. J. Hepatol. 58, 297–305. 10.1016/j.jhep.2012.10.002 [PubMed: 23046676]

Asghar Z, Yau D, Chan F, LeRoith D, Chan CB, Wheeler MB, 2006. Insulin resistance causes increased beta-cell mass but defective glucose-stimulated insulin secretion in a murine model of type 2 diabetes. Diabetologia 49, 90–99. 10.1007/s00125-005-0045-y [PubMed: 16362284]

Back SH, Kaufman RJ, 2012. Endoplasmic reticulum stress and type 2 diabetes. Annu. Rev. Biochem. 81, 767–793. 10.1146/annurev-biochem-072909-095555 [PubMed: 22443930]

Butler AE, Janson J, Bonner-Weir S, Ritzel R, Rizza RA, Butler PC, 2003. Beta-cell deficit and increased beta-cell apoptosis in humans with type 2 diabetes. Diabetes 52, 102–110. [PubMed: 12502499]

Champy M-F, Selloum M, Zeitler V, Caradec C, Jung B, Rousseau S, Pouilly L, Sorg T, Auwerx J, 2008. Genetic background determines metabolic phenotypes in the mouse. Mamm. Genome 19, 318–331. 10.1007/s00335-008-9107-z [PubMed: 18392653]

Charron MJ, Brosius FC, Alper SL, Lodish HF, 1989. A glucose transport protein expressed predominately in insulin-responsive tissues. Proc. Natl. Acad. Sci. 86, 2535–2539. 10.1073/pnas.86.8.2535 [PubMed: 2649883]

Davis J, Kwong JQ, Kitsis RN, Molkentin JD, 2013. Apoptosis Repressor with a CARD Domain (ARC) Restrains Bax-Mediated Pathogenesis in Dystrophic Skeletal Muscle. PLoS ONE 8. 10.1371/journal.pone.0082053

Geertman R, McMahon A, Sabban EL, 1996. Cloning and characterization of cDNAs for novel proteins with glutamic acid-proline dipeptide tandem repeats. Biochim. Biophys. Acta 1306, 147–152. [PubMed: 8634331]

Gupta D, Jetton TL, LaRock K, Monga N, Satish B, Lausier J, Peshavaria M, Leahy JL, 2017. Temporal characterization of β cell-adaptive and -maladaptive mechanisms during chronic high-fat feeding in C57BL/6NTac mice. J. Biol. Chem. 292, 12449–12459. 10.1074/jbc.M117.781047 [PubMed: 28487366]

Gustafsson AB, Tsai JG, Logue SE, Crow MT, Gottlieb RA, 2004. Apoptosis repressor with caspase recruitment domain protects against cell death by interfering with Bax activation. J. Biol. Chem. 279, 21233–21238. 10.1074/jbc.M400695200 [PubMed: 15004034]

Heydemann A, 2016. An Overview of Murine High Fat Diet as a Model for Type 2 Diabetes Mellitus. J. Diabetes Res. 2016. 10.1155/2016/2902351

Hull RL, Westermark GT, Westermark P, Kahn SE, 2004. Islet amyloid: a critical entity in the pathogenesis of type 2 diabetes. J. Clin. Endocrinol. Metab. 89, 3629–3643. 10.1210/jc.2004-0405 [PubMed: 15292279]

Hull RL, Willard JR, Struck MD, Barrow BM, Brar GS, Andrikopoulos S, Zraika S, 2017. High fat feeding unmasks variable insulin responses in male C57BL/6 mouse substrains. J. Endocrinol. 233, 53–64. 10.1530/JOE-16-0377 [PubMed: 28138002]

Ikemoto S, Takahashi M, Tsunoda N, Maruyama K, Itakura H, Ezaki O, 1996. High-fat diet-induced hyperglycemia and obesity in mice: differential effects of dietary oils. Metabolism. 45, 1539–1546. 10.1016/s0026-0495(96)90185-7 [PubMed: 8969289]

James DE, Brown R, Navarro J, Pilch PF, 1988. Insulin-regulatable tissues express a unique insulin-sensitive glucose transport protein. Nature 333, 183–185. 10.1038/333183a0 [PubMed: 3285221]

Jang T, Kim SH, Jeong J-H, Kim S, Kim Y-G, Kim YG, Park HH, 2015. Crystal structure of caspase recruiting domain (CARD) of apoptosis repressor with CARD (ARC) and its implication in inhibition of apoptosis. Sci. Rep. 5. 10.1038/srep09847

Jo D-G, Jun J-I, Chang J-W, Hong Y-M, Song S, Cho D-H, Shim SM, Lee H-J, Cho C, Kim DH, et al. , 2004. Calcium binding of ARC mediates regulation of caspase 8 and cell death. Mol. Cell. Biol. 24, 9763–9770. 10.1128/MCB.24.22.9763-9770.2004 [PubMed: 15509781]

Jurgens CA, Toukatly MN, Fligner CL, Udayasankar J, Subramanian SL, Zraika S, Aston-Mourney K, Carr DB, Westermark P, Westermark GT, et al. , 2011. β-cell loss and β-cell apoptosis in human type 2 diabetes are related to islet amyloid deposition. Am. J. Pathol. 178, 2632–2640. 10.1016/j.ajpath.2011.02.036 [PubMed: 21641386]

Koseki T, Inohara N, Chen S, Núñez G, 1998. ARC, an inhibitor of apoptosis expressed in skeletal muscle and heart that interacts selectively with caspases. Proc. Natl. Acad. Sci. U. S. A. 95, 5156–5160. [PubMed: 9560245]

Kung G, Dai P, Deng L, Kitsis RN, 2014. A novel role for the apoptosis inhibitor ARC in suppressing TNFα-induced regulated necrosis. Cell Death Differ. 21, 634–644. 10.1038/cdd.2013.195 [PubMed: 24440909]

Li Y-Z, Lu D-Y, Tan W-Q, Wang J-X, Li P-F, 2008. p53 initiates apoptosis by transcriptionally targeting the antiapoptotic protein ARC. Mol. Cell. Biol. 28, 564–574. 10.1128/MCB.00738-07 [PubMed: 17998337]

Liu X, Tamada K, Kishimoto R, Okubo H, Ise S, Ohta H, Ruf S, Nakatani J, Kohno N, Spitz F, et al. , 2015. Transcriptome profiling of white adipose tissue in a mouse model for 15q duplication syndrome. Genomics Data 5, 394–396. 10.1016/j.gdata.2015.06.035 [PubMed: 26484295]

Marchetti P, Bugliani M, Lupi R, Marselli L, Masini M, Boggi U, Filipponi F, Weir GC, Eizirik DL, Cnop M, 2007. The endoplasmic reticulum in pancreatic beta cells of type 2 diabetes patients. Diabetologia 50, 2486–2494. 10.1007/s00125-007-0816-8 [PubMed: 17906960]

McKimpson WM, Weinberger J, Czerski L, Zheng M, Crow MT, Pessin JE, Chua SC, Kitsis RN, 2013. The apoptosis inhibitor ARC alleviates the ER stress response to promote β-cell survival. Diabetes 62, 183–193. 10.2337/db12-0504 [PubMed: 22933109]

McKimpson WM, Zheng M, Chua SC, Pessin JE, Kitsis RN, 2017. ARC is essential for maintaining pancreatic islet structure and β-cell viability during type 2 diabetes. Sci. Rep. 7, 7019. 10.1038/s41598-017-07107-w [PubMed: 28765602]

Min SY, Desai A, Yang Z, Sharma A, Genga RMJ, Kucukural A, Lifshitz L, Maehr R, Garber M, Corvera S, 2019. Multiple human adipocyte subtypes and mechanisms of their development (preprint). Physiology. 10.1101/537464

Mosser RE, Maulis MF, Moullé VS, Dunn JC, Carboneau BA, Arasi K, Pappan K, Poitout V, Gannon M, 2015. High-fat diet-induced β-cell proliferation occurs prior to insulin resistance in C57Bl/6J male mice. Am. J. Physiol. - Endocrinol. Metab. 308, E573–E582. 10.1152/ajpendo.00460.2014 [PubMed: 25628421]

Nam Y-J, Mani K, Ashton AW, Peng C-F, Krishnamurthy B, Hayakawa Y, Lee P, Korsmeyer SJ, Kitsis RN, 2004. Inhibition of both the extrinsic and intrinsic death pathways through nonhomotypic death-fold interactions. Mol. Cell 15, 901–912. 10.1016/j.molcel.2004.08.020 [PubMed: 15383280]

Neuss M, Monticone R, Lundberg MS, Chesley AT, Fleck E, Crow MT, 2001. The Apoptotic Regulatory Protein ARC (Apoptosis Repressor with Caspase Recruitment Domain) Prevents Oxidant Stress-mediated Cell Death by Preserving Mitochondrial Function. J. Biol. Chem. 276, 33915–33922. 10.1074/jbc.M104080200 [PubMed: 11438535]

Omikorede O, Qi C, Gorman T, Chapman P, Yu A, Smith DM, Herbert TP, 2013. ER stress in rodent islets of Langerhans is concomitant with obesity and β-cell compensation but not with β-cell dysfunction and diabetes. Nutr. Diabetes 3, e93–e93. 10.1038/nutd.2013.35 [PubMed: 24145577]

Özcan U, Cao Q, Yilmaz E, Lee A-H, Iwakoshi NN, Özdelen E, Tuncman G, Görgün C, Glimcher LH, Hotamisligil GS, 2004. Endoplasmic Reticulum Stress Links Obesity, Insulin Action, and Type 2 Diabetes. Science 306, 457–461. 10.1126/science.1103160 [PubMed: 15486293]

Paschen M, Moede T, Valladolid-Acebes I, Leibiger B, Moruzzi N, Jacob S, García-Prieto CF, Brismar K, Leibiger IB, Berggren P-O, 2019. Diet-induced β-cell insulin resistance results in reversible loss of functional β-cell mass. FASEB J. 33, 204–218. 10.1096/fj.201800826R [PubMed: 29957055]

Rahier J, Guiot Y, Goebbels RM, Sempoux C, Henquin JC, 2008. Pancreatic beta-cell mass in European subjects with type 2 diabetes. Diabetes Obes. Metab. 10 Suppl 4, 32–42. 10.1111/j.1463-1326.2008.00969.x [PubMed: 18834431]

Rosell M, Kaforou M, Frontini A, Okolo A, Chan Y-W, Nikolopoulou E, Millership S, Fenech ME, MacIntyre D, Turner, et al. , 2014. Brown and white adipose tissues: intrinsic differences in gene expression and response to cold exposure in mice. Am. J. Physiol.-Endocrinol. Metab. 306, E945–E964. 10.1152/ajpendo.00473.2013 [PubMed: 24549398]

Surwit RS, Kuhn CM, Cochrane C, McCubbin JA, Feinglos MN, 1988. Diet-Induced Type II Diabetes in C57BL/6J Mice. Diabetes 37, 1163–1167. 10.2337/diab.37.9.1163 [PubMed: 3044882]

Templin AT, Samarasekera T, Meier DT, Hogan MF, Mellati M, Crow MT, Kitsis RN, Zraika S, Hull RL, Kahn SE, 2017. Apoptosis Repressor with Caspase Recruitment Domain Ameliorates Amyloid-Induced β-Cell Apoptosis and JNK Pathway Activation. Diabetes. 10.2337/db16-1352

Tschöp MH, Speakman JR, Arch JRS, Auwerx J, Brüning JC, Chan L, Eckel RH, Farese RV, Galgani JE, Hambly C, et al. , 2011. A guide to analysis of mouse energy metabolism. Nat. Methods 9, 57–63. 10.1038/nmeth.1806 [PubMed: 22205519]

Winzell MS, Ahrén B, 2004. The High-Fat Diet–Fed Mouse: A Model for Studying Mechanisms and Treatment of Impaired Glucose Tolerance and Type 2 Diabetes. Diabetes 53, S215–S219. 10.2337/diabetes.53.suppl_3.S215 [PubMed: 15561913]

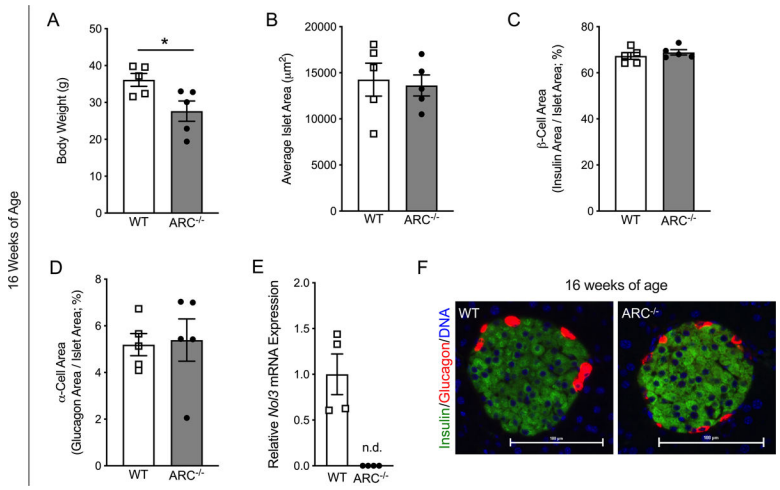

Figure 1: 16-week-old ARC$^{-/-}$ mice fed NCD display reduced body weight and unaltered islet morphology compared to WT mice.

(A) Body weight was reduced in ARC$^{-/-}$ (closed circles) versus WT mice (open squares). (B) Islet area, (C) β-cell area (insulin/islet area), and (D) α-cell area (glucagon/islet area) were not different between NCD fed wild type (WT) (open squares) and ARC$^{-/-}$ mice (closed circles) at 16-weeks-of-age. (E) *Nol3* mRNA, the transcript for ARC, was not detectable in ARC$^{-/-}$ (closed circles) compared to WT (open squares) mouse islets. Data are normalized to *18S* rRNA levels and expressed as fold relative to WT using the ΔΔCT method. (F) Representative images from WT and ARC$^{-/-}$ islets are shown. Scale bar = 100 μm. n=4–5/genotype. *p<0.05.

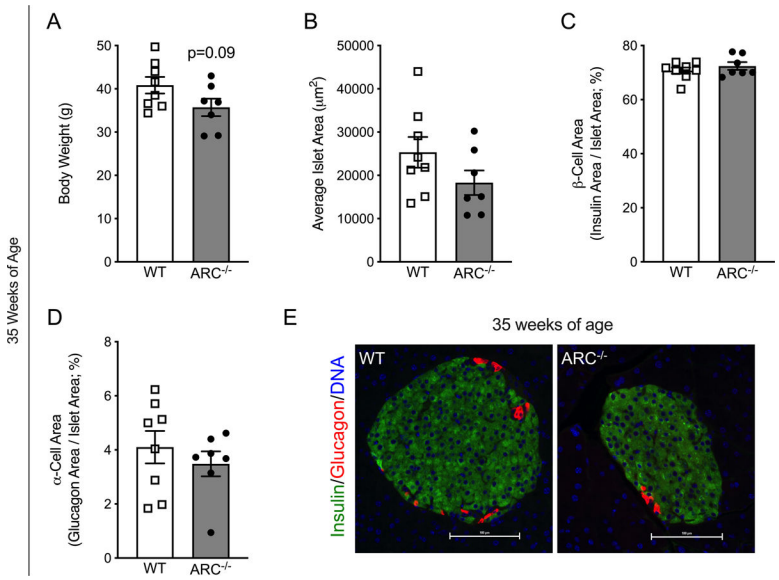

Figure 2: 35-week-old ARC$^{-/-}$ mice fed NCD display unaltered body weight and islet morphology compared to WT mice.

(A) Body weight, (B) islet area, (C) β-cell area (insulin/islet area), and (D) α-cell area (glucagon/islet area) were not different between NCD fed wild type (WT) (open squares) and ARC$^{-/-}$ (closed circles) mice at 35-weeks-of-age. (E) Representative images from WT and ARC$^{-/-}$ islets are shown. Scale bar = 100 μm. n=7–8/genotype.

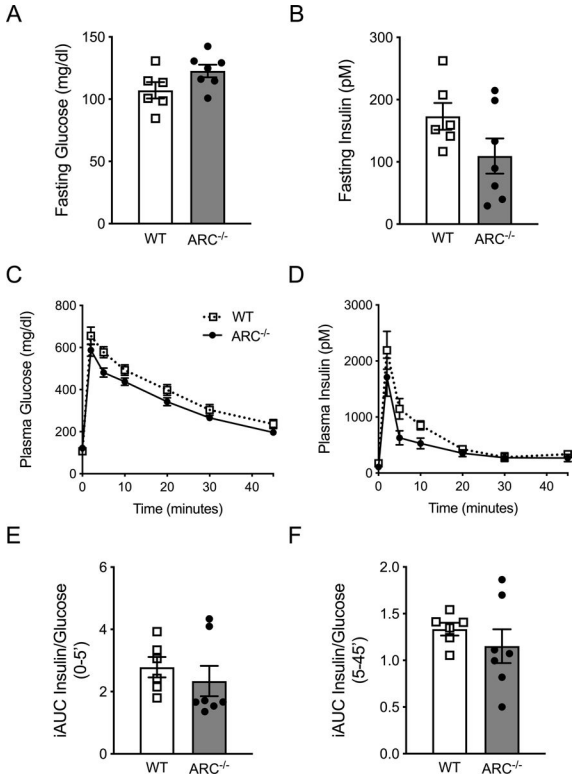

Figure 3: 35-week-old ARC$^{-/-}$ mice fed NCD display unaltered fasting and glucose-stimulated plasma glucose and insulin levels compared to WT mice.

(A) Fasting plasma glucose and (B) fasting plasma insulin were not different between 35-week-old wild type (WT) (open squares) and ARC$^{-/-}$ (closed circles) mice fed a normal chow diet (NCD). Intravenous glucose (1 g/kg body weight) stimulated (C) plasma glucose and (D) plasma insulin were not different between genotypes. In response to intravenous glucose stimulation, the change in insulin as a function of the change in glucose (iAUC insulin/iAUC glucose) was not different between WT (open squares) and ARC$^{-/-}$ mice (closed circles) (E) from 0 to 5 or (F) from 5 to 45 minutes. n=6–7/genotype.

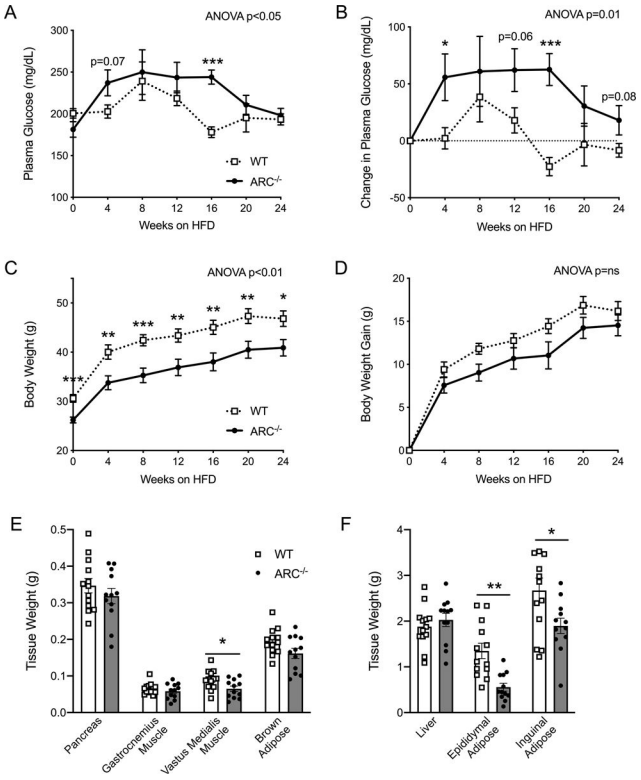

Figure 4: ARC$^{-/-}$ mice fed HFD exhibit transient worsening of hyperglycemia and reduced body weight compared to WT mice.

Wild type (WT, open squares) and ARC$^{-/-}$ mice (closed circles) were fed a high fat diet (HFD) for 24 weeks and evaluated every 4 weeks. (A) Non-fasting plasma glucose was elevated to similar levels in both genotypes but remained elevated in ARC$^{-/-}$ mice (closed circles) after 16 weeks of HFD feeding when WT mice (open squares) glucose had normalized. (B) ARC$^{-/-}$ mice exhibited a significantly greater change in plasma glucose after 4 weeks of HFD feeding. (C) ARC$^{-/-}$ mice (closed circles) displayed significantly reduced body weight throughout the HFD feeding study, but (D) body weight gain was not different from WT mice (open squares). Following 24 weeks of high fat diet (HFD) feeding, ARC$^{-/-}$ mice (closed circles) display (E) decreased vastus medialis muscle, (F) epididymal adipose and inguinal adipose tissue mass compared to WT mice (open squares). n=12–13/genotype. *p<0.05, **p<0.01, ***p<0.001

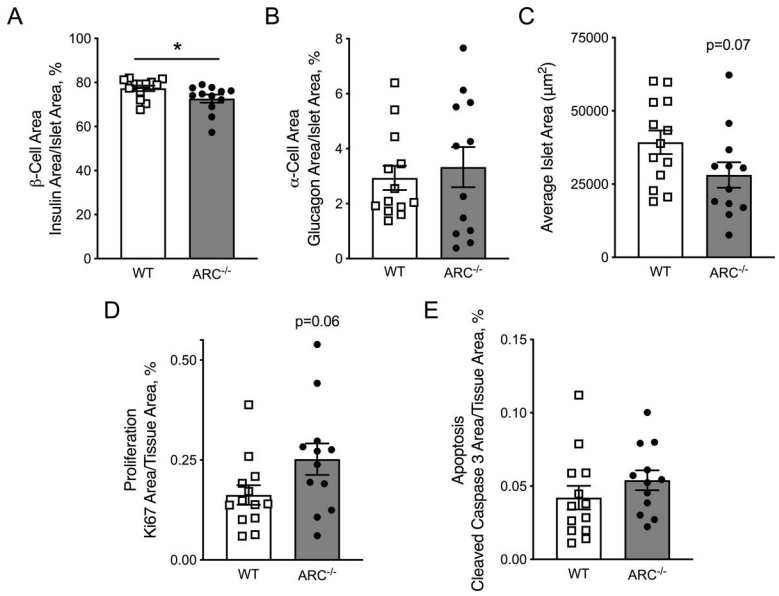

Figure 5: 35-week-old ARC$^{-/-}$ mice fed HFD for 24 weeks display reduced β-cell area but no differences in α-cell area, islet area, proliferation or apoptosis compared to WT mice.

Following the HFD feeding study period, (A) β-cell area (insulin/islet area) was reduced in ARC$^{-/-}$ (closed circles) versus wild type (WT, open squares) mice. (B) α-cell area (glucagon/islet area), (C) average islet area, (D) Ki67 area and (E) cleaved caspase 3 area were not significantly different between WT (open squares) and ARC$^{-/-}$ (closed circles) mice. n=12–13/genotype. *p<0.05

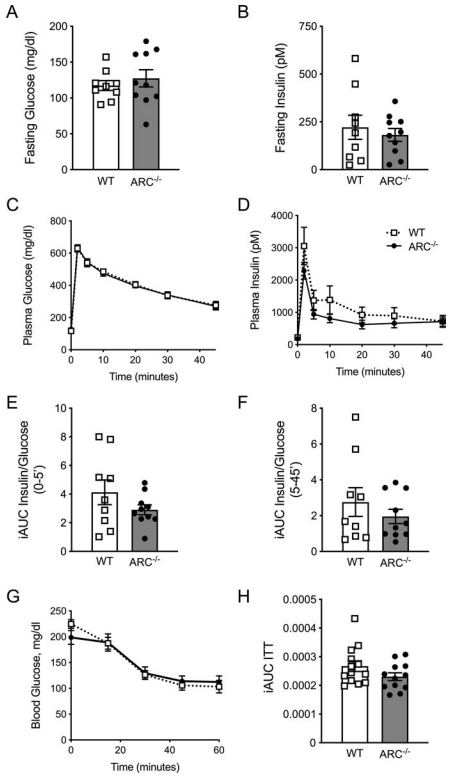

Figure 6: 35-week-old ARC$^{-/-}$ mice fed HFD for 24 weeks display unaltered fasting and glucose-stimulated plasma glucose and insulin concentrations, and unaltered insulin sensitivity compared to WT mice.

Following 24 weeks of high fat diet (HFD) feeding, (A) fasting plasma glucose and (B) fasting plasma insulin were not different between wild type (WT, open squares) and ARC$^{-/-}$ (closed circles) mice. Intravenous glucose (1 g/kg body weight) stimulated (C) plasma glucose and (D) plasma insulin were not different between genotypes. In response to intravenous glucose stimulation, the change in insulin as function of the change in glucose (iAUC insulin/iAUC glucose) was not different between WT (open squares) and ARC$^{-/-}$ (closed circles) mice (E) from 0 to 5 or (F) from 5 to 45 minutes. (G) Insulin administered at a dose of 1 U/kg body weight reduced absolute plasma glucose levels to similar degrees in wild type (WT, open squares) and ARC$^{-/-}$ mice (closed circles) following HFD feeding. (H) Inverse area under the curve (iAUC) of glucose in response to insulin was not different between WT (open squares) and ARC$^{-/-}$ (closed circles) mice. (A-F) n=9–10/genotype, (G-H) n=12–13/genotype.